1995-12-01

Ponticulin plays a role in the positional stabilization of pseudopods

D. C. Shutt

Et al.

Ponticulin Plays a Role in the Positional Stabilization of Pseudopods

Damon C. Shutt,* Deborah Wessels,* Keith Wagenknecht,* Anand Chandrasekhar,* Anne L. Hitt,‡ Elizabeth J. Luna,‡ and David R. Soll*

*Department of Biological Sciences, University of Iowa, Iowa City, Iowa 52242; and ‡Cell Biology Group, Worcester Foundation for Biomedical Research, Shrewsbury, Massachusetts 01545

Abstract. Ponticulin is a 17-kD glycoprotein that represents a major high affinity link between the plasma membrane and the cortical actin network of *Dictyostelium.* To assess the role of ponticulin in pseudopod extension and retraction, the motile behavior of two independently generated mutants lacking ponticulin was analyzed using computer-assisted two- and three-dimensional motion analysis systems. More than half of the lateral pseudopods formed off the substratum by ponticulin-minus cells slipped relative to the substratum during extension and retraction. In contrast, all pseudopods formed off the substratum by wild-type cells were positionally fixed in relation to the substratum. Ponticulin-minus cells also formed a greater proportion of both anterior and lateral pseudopods off the substratum and absorbed a greater proportion of lateral pseudopods into the uropod than wild-type cells. In a spatial gradient of cAMP, ponticulin-minus cells were less efficient in tracking the source of chemoattractant. Since ponticulin-minus cells extend and retract pseudopods with the same time course as wild-type cells, these behavioral defects in ponticulin-minus cells appear to be the consequence of pseudopod slippage. These results demonstrate that pseudopods formed off the substratum by wild-type cells are positionally fixed in relation to the substratum, that ponticulin is required for positional stabilization, and that the loss of ponticulin and the concomitant loss of positional stability of pseudopods correlate with a decrease in the efficiency of chemotaxis.

DIRECTED cell movement plays a key role in multicellular morphogenesis, in wound repair, and in cellular immunity. The motility of the cells responsible for these processes involves complex three-dimensional changes in cell morphology, the most important of which are the extension and retraction of pseudopods or lamellipods (Abercrombie et al., 1970*a*,*b*; Murray et al., 1992; Wessels et al., 1994; Soll, 1995). Pseudopod extension in human polymorphonuclear leukocytes and in *Dictyostelium* amoebae has been shown to occur both on and off the substratum (Murray et al., 1992; Wessels et al., 1994; Schindl et al., 1995). In *Dictyostelium*, it has been demonstrated that interactions between the substratum and the ventral surface of a pseudopod promote cell turning (Wessels et al., 1994; Soll, 1995). Although lateral pseudopods formed off the substratum do not usually promote turns, in gradients of chemoattractant they may be important components of the mechanism by which eukaryotic cells sense the gradient (Varnum-Finney et al., 1987*a*,*b*; Wessels et al., 1994; Soll, 1995). The spatial and temporal dynamics of receptor occupancy on pseudopods may effect very specific changes in the actin-based cytoskeleton, which then leads to continued pseudopod extension or retraction (Varnum-Finney et al., 1987*a*,*b*; Caterina and Devreotes, 1991; Condeelis et al., 1992; Condeelis, 1993; Downey, 1994).

The transmembrane protein, ponticulin, is the major high affinity link between the actin cytoskeleton and the plasma membrane of *Dictyostelium* (Wuestehube and Luna, 1987; Wuestehube et al., 1989; Chia et al., 1991; Hitt et al., 1994*b*). One of the few membrane proteins known to contain both a cytoplasmic domain and a glycosyl anchor (Hitt et al., 1994*a*), ponticulin is a 17-kD glycoprotein that accounts for 96% of the in vitro actin-binding activity and virtually all of the actin nucleation activity of isolated plasma membranes (Wuestehube and Luna 1987; Luna et al., 1990; Shariff and Luna, 1990; Hitt et al., 1994*b*). Thus, the localization and function of this protein suggest that it should play a fundamental role in pseudopod extension and cellular motility.

Genetic ablation of ponticulin results in cells that contain little membrane-bound actin and exhibit defects in multicellular development under select conditions (Hitt et al., 1994*b*). Surprisingly, ponticulin-minus mutants are still capable of aggregating and progressing through morphogenesis (Hitt et al., 1994*b*), suggesting that ponticulin is not essential for cellular translocation. However, it has become increasingly clear that many actin-associated proteins are not essential for the basic capacity of a cell to ex-

Address all correspondence to Dr. David R. Soll, Department of Biological Sciences, University of Iowa, Iowa City, IA 52242. Tel.: (319) 335-1117. Fax: (319) 335-2772.

A. Chandrasekhar's current address is Department of Biology, University of Michigan, Ann Arbor, MI 48109-1048.

tend a pseudopod and crawl, but are required for the orderly and highly regulated temporal and spatial dynamics of anterior and lateral pseudopod extension and retraction (for review see Soll, 1995). The selective absence of such proteins, effected by gene disruption, can result in abnormalities in the frequency, order, rate of growth and 3-D geometry of pseudopod extension and retraction (Wessels et al., 1988, 1989, 1991, 1996; Wessels and Soll, 1990; Titus et al., 1993). These abnormalities, in turn, can impact significantly on the efficiency of translocation, chemotaxis, and multicellular morphogenesis (DeLozanne and Spudich, 1987; Knecht and Loomis, 1987; Wessels et al., 1988; Condeelis, 1993; Doolittle et al., 1995; Sheldon and Knecht, 1995).

To assess directly the role of ponticulin in single cell motility and chemotaxis, we have used computer-assisted two- and three-dimensional motion analysis systems (Soll, 1988, 1995; Soll et al., 1988; Murray et al., 1992; Wessels et al., 1994; Chandrasekhar et al., 1995) to characterize the motile behavior of aggregation-competent ponticulin-minus cells in buffer and in spatial gradients of cAMP. We have discovered that all lateral pseudopods formed off the substratum by wild-type cells in buffer are fixed positionally in relation to the substratum during extension and retraction, while more than half of the lateral pseudopods formed by ponticulin-minus cells in buffer are not fixed and slip posteriorly along the cell axis. Slippage is very rapid, and results in an abnormally high proportion of pseudopods that are retracted into the uropod rather than into the main cell body. Ponticulin-minus cells also form an abnormally high proportion of both anterior and lateral pseudopods off the substratum, and these cells are less efficient at chemotaxing in a spatial gradient of the chemoattractant, cAMP. Our results demonstrate that ponticulin plays a novel role in the control of pseudopod position relative to the substratum, and that this spatial stability is an important component of normal cell motility and chemotaxis.

Materials and Methods

Ponticulin-Minus Mutants

The genesis of the ponticulin-minus mutants, Tf1.1 and Tf24.1, in *Dictyostelium discoideum* strain Ax3K was described in detail in a previous report (Hitt et al., 1994*a*). In brief, mutants were generated by homologous recombination with a construct in which a neomycin-resistance cassette was inserted after nucleotide 9 of the ponticulin coding sequence. The single-copy gene encoding ponticulin was disrupted in both of the independently generated transformant cell lines, as demonstrated by Southern blot hybridization and by the absence of a diagnostic 2.5-kb PCR product (Hitt et al., 1994*a*). Northern and Western analyses of Tf1.1 and Tf24.1 confirmed the absence of detectable ponticulin message and ponticulin protein, respectively (Hitt et al., 1994*a*). Both mutant cell lines were subcloned twice in HL-5 medium (Cocucci and Sussman, 1970) and stored as frozen stocks in HL-5 medium containing 10% dimethylsulfoxide.

Development of Wild-type and Mutant Strains

Cells from frozen cultures were grown in suspension in HL-5 medium at 22°C and serially transferred for no longer than 3 wk. To initiate development, cells from the mid–log phase of growth were washed free of nutrient medium with a buffered salt solution (BSS)[1] consisting of 20 mM KCl, 2.4 mM $MgCl_2$, 0.34 mM streptomycin sulfate, 20 mM KH_2PO_4, and 20 mM Na_2HPO_4, pH 6.4 (Sussman, 1987). Cells in BSS were dispersed at high density (5×10^6 cells per cm^2) on a black filter (29; Whatman Inc., Clifton, NJ) supported by two prefilters (Millipore Corp., Bedford, MA) saturated with the same solution (Soll, 1987). These conditions, in which cells are multilayered, have been shown to result in highly synchronous development and highly reproducible developmental timing of Ax3 cells (Soll, 1979). Unless otherwise noted, cells of both wild-type and mutant strains were removed at the ripple stage, which represents the onset of aggregation under these conditions (Soll, 1979), by gently pipetting BSS across the surface of the development filter. The cells were pelleted and washed, and the final cell suspension, in BSS, was gently mixed and adjusted to a concentration of 3×10^4 cells per ml for inoculation into a perfusion or chemotaxis chamber. Growth cultures of strain Ax2 and strain Ax3-clone RC3 were initiated from desiccated cultures of spores and then developed in the same manner as described above.

Two-Dimensional Analysis of Cell Behavior and Pseudopod Dynamics

A 0.3-ml aliquot of cell suspension was inoculated into a Dvorak-Stotler chamber (Nicholson Precision Instruments, Inc., Gaithersburg, MD), the chamber closed, and the cells allowed to settle to the bottom glass chamber wall to reinitiate motile behavior. The resulting density on the chamber wall was ~33 cells/mm^2. The chamber was then clamped to the stage of an inverted microscope (ICM 405; Carl Zeiss, Inc., Thornwood, NY) equipped with differential interference contrast (DIC) optics for high magnification (×630) recordings. The chamber was perfused with BSS, and the behavior of single cells not in contact with each other videorecorded on half or three-quarter inch tape according to methods previously described (Wessels et al., 1989; Wessels and Soll, 1990). Low magnification videorecorded cell images were automatically digitized and high magnification cell images were manually digitized into the data file of the DIAS program (Wessels et al., 1992; Sylwester et al., 1993, 1995). 2-D motility and morphology parameters were computed according to formulas and methods previously described (Soll, 1988, 1995; Soll et al., 1988). Instantaneous velocity for a cell in frame (n) was computed by first drawing a line from the cell centroid in the previous frame ($n - 1$) to the cell centroid in the subsequent frame ($n + 1$), and dividing the length of the line by $2\Delta t$, where Δt is the time interval between analyzed frames. Positive flow was computed as the percentage of area contained in the expansion zones of difference pictures, generated by overlapping the images in frames n and $n - 1$ (Soll, 1995). Roundness was computed as $(4\pi \times \text{area}/\text{perimeter}^2) \times 100$. A perfect circle has a roundness measure of 100% and a straight line a roundness measure of 0%. 2-D centroid tracks were analyzed for turning frequency by dividing total translocation time by the number of turns persisting for ≥32 s that caused the direction of the cell centroid to change by ≥30°.

Definition of a Pseudopod

In the 2-D analysis of the spatial and temporal dynamics of pseudopod extension and retraction, an anterior pseudopod was defined as a cell extension that formed at the anterior end of the main cell body in the approximate direction (± 30°) of the long cell axis, which attained a minimum area of 4 μm^2 and which was initially free of particulate cytoplasm. The anterior end of a cell was determined from the long axis of the cell established during the preceding translocation step in the behavior cycle (Wessels et al., 1994). A lateral pseudopod was defined as an extension which formed from the side of the cell body in a direction 30° to 90° from the long cell axis, which attained a minimum area of 4 μm^2 and which was initially free of particulate cytoplasm. Again, the angle of pseudopod expansion was determined from the long axis of the cell established during the preceding translocation step. Comparisons of the videotaped segments of cells recorded through DIC optics and the digitized images of the same cells demonstrated that in all cases pseudopods defined by the preceding criteria in digitized images represented cell extensions in which the apical zones were free of particles. As pseudopods grew, the apical ends remained particle free, but the proximal regions filled with particulate cytoplasm. The apical zones of particle-free cytoplasm corresponded to the F-actin–filled zones of pseudopods, as determined by staining with fluorescein-conjugated phalloidin (Wessels et al., 1989). During pseudopod retraction, the pseudopods were primarily filled with particulate cytoplasm.

1. *Abbreviations used in this paper*: BSS, buffered salt solution; CI, chemotactic index; DIC, differential interference contrast.

Three-Dimensional Analysis of Cell Behavior and Pseudopod Dynamics

The methods for optically sectioning living cells, reconstructing 3-D images and wrapping the images for analysis with 3-D DIAS software have been described elsewhere (Murray et al., 1992; Wessels et al., 1994; Soll, 1995). In brief, cells were inoculated into a Dvorak-Stotler chamber, and the chamber was positioned on the stage of a Zeiss ICM405 inverted microscope equipped with DIC optics and perfused with BSS. To obtain optical sections, the plane of focus was automatically raised in 1-μm increments at 0.2-s intervals using a newly developed microstepper motor regulated by a Macintosh-based operating program. Sectioning of a cell was complete in 2 s and repeated every 5 s. Perimeters of the in-focus portion of each section were manually digitized into the 3-D DIAS data file.

To illustrate this technique, the original videorecorded DIC images and the manually digitized perimeters of in-focus portions are presented in Fig. 1 *A* for one 3-D image (i.e., at a single time point). Pseudo–3-D representations of the stacked optical sections are presented at progressive angles in Fig. 1 *B*. A more representative rendition of the reconstructed cell was then generated by reinserting the in-focus portion of each image into its digitized perimeter, stacking these images and presenting them as pseudo–3-D renditions at progressive angles in Fig. 1 *C*. Noise removal and dilation-erosion techniques were used to unify perimeters, when necessary, in each optical section, and final shapes were generated using β-splines (Soll, 1995). The final shapes in the stack of optical sections were first connected to form transparent caged images (Fig. 1 *D*), then wrapped and smoothed to generate nontransparent 3-D reconstructions that most closely reflect the original images (Fig. 1 *E*). Smoothed images of cells reconstructed at 5-s intervals were then viewed as dynamic animations on the polarizing screen of a stereo monitor (4337; Tektronix, Beaverton, OR). The final 3-D reconstructions were used to quantitate 3-D parameters.

In 3-D analyses of pseudopod extension and retraction, the criteria used to define anterior and lateral pseudopods were similar to those used in 2-D analyses. However, instead of using minimum area as a criterion, a minimum vol of 6 μm^3 was used, and instead of using 2-D shape criteria, 3-D shape criteria were used to interpret extensions. Comparisons of 3-D reconstructions with the original DIC optical sections demonstrated that pseudopods defined by 3-D criteria conformed to the same criteria used in defining a pseudopod in 2-D images.

Pseudopod volume was measured in μm^3 by encapsulating the 3-D projection in a box which abutted the cell body and then summing the faceted blocks contained in a faceted image of the pseudopod (Wessels et al., 1996). Rates of expansion or contraction were computed in μm^3 per 5 s.

Error Estimates

To estimate the error in 3-D measurements due to movement of the cell or pseudopod during optical sectioning, we first computed the distance an average cell would move in the course of 2 s, the time required to generate a 3-D image. For an average cell moving 10 μm/min, the distance moved in 2 s is 0.33 μm. Since elongate cells are, on average, 20 μm in length, the directional skew (the distance error between the bottom and top section due to movement during optical reconstruction) is ~2%. For a pseudopod growing at an average rate of 30 μm/min with an average height of 4 μm, the average number of optical sections necessary for reconstruction is four, and the average time for reconstruction is 0.8 s. In this case, the directional skew would be ~10% between the bottom and top sections of the reconstruction.

To estimate volume errors due to missing portions of the pseudopod in optical sections, we modeled a pseudopod as a parabola, then positioned the parabola in the worst positions for analysis (i.e., with the highest and lowest optical sections just missing the top and bottom edges of the pseudopod, respectively). For an average-sized pseudopod 5 μm in length and 4 μm in height, the average error is 12%. This low error is due to an automatic interpolation algorithm in the 3D-DIAS program which completes shapes for volume measurements.

To test the reliability and accuracy of in-focus outlining, an Ax3K cell was fixed on a gridded coverslip and optically sectioned at 1-μm increments using the DIC method. The cell was then stained with FITC-conjugated phalloidin, which stains F-actin, but more importantly, provides a high resolution image of F-actin just under the plasma membrane and, therefore, a very accurate outline of the cell. The original cell optically sectioned by DIC was found on the gridded coverslip and optically resectioned by confocal microscopy. In the confocal microscopy sectioning procedure, 40 sections at 0.2-μm increments were collected. The in-focus perimeters of the DIC sections and the perimeters of the confocal sections were then both digitized into the DIAS data bank. Both the reconstructed DIC and confocal pseudo–3-D images were then generated, and their volumes compared. The reconstructed images were visually similar and the difference in computed volume was only 0.4%. The only difference between the two reconstructions was the resolution of a small number of stained filopodia in the confocal reconstruction.

Analysis of Chemotaxis in a Gradient Chamber

To assess the chemotactic index (CI) of individual parental Ax3K and mu-

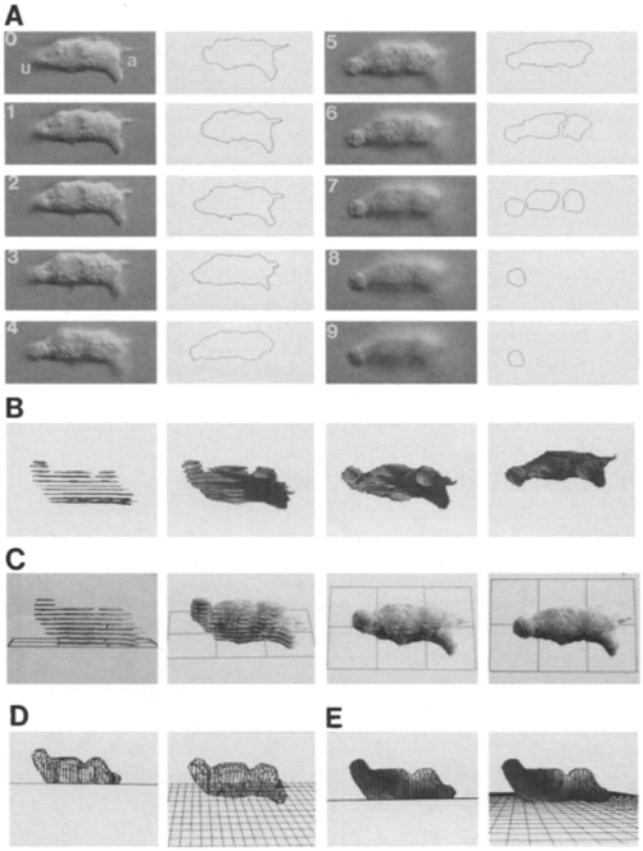

Figure 1. Optical sectioning and computer-generated reconstruction of a translocating cell at a single time point. (*A*) The original sequence of optical sections obtained by differential interference contrast microscopy and manually drawn perimeters of the in-focus image. Sections were recorded at 0.2-s intervals and were separated in the z-axis by 1 μm. 0 is at the glass substratum and 9 is 9 μm above the substratum. (*B*) The digitized perimeters of the in-focus portions of the optical sections are filled and stacked to create a pseudo 3-D reconstruction. This reconstruction is then rotated for views initially from the side and progressively toward the dorsal surface. (*C*) Each digitized perimeter of the in-focus portion of the optical sections are refilled with only that portion of the section which was in focus, and these filled perimeters are stacked and viewed from progressively dorsal angles. This provides a more realistic reconstruction. (*D*) The plates in the image in *B* are connected by facets. This transparent image is used for computing 3-D morphology and motility parameters (Soll, 1995). Two views are presented of the faceted image. (*E*) The faceted image is then smoothed and wrapped to obtain a nontransparent image which most closely represents the original cell. Two views are presented of the wrapped image. *a*, anterior end of cell; *u*, uropod.

tant cells in a spatial gradient of the chemoattractant cAMP, a dilute suspension of cells in BSS was dispersed on the bridge of a gradient chamber which consisted of a 2-mm plexiglass bridge bordered on either side by parallel troughs that were 2 mm wide and 1 mm deep (Zigmond, 1977; Varnum and Soll, 1984; Varnum-Finney et al., 1987*b*). BSS containing 1.0 μM cAMP was placed in the trough serving as the "source," and BSS alone was placed in the trough serving as the "sink" (Varnum and Soll, 1984; Varnum-Finney et al., 1987*b*). Cells were allowed to acclimate for 4 min and were then videorecorded for 12 min. The CI of a cell was computed from the centroid track as the directional distance (net distance toward the source) divided by the total distance traveled (McCutcheon, 1946; Varnum and Soll, 1984). A CI of 0 reflects no net movement towards or away from the source of attractant; a CI of +1.0 reflects persistent movement directly towards the source (i.e., up the gradient); and a CI of −1.0 reflects persistent movement directly away from the source (i.e., down the gradient). All cells analyzed were separated from other cells on the bridge by at least two cell body lengths.

Results

Developmental Regulation of Motility

Since the rate of single cell motility is regulated by the developmental program of *Dictyostelium* (Varnum et al., 1986), we first identified conditions that permitted comparison of wild-type Ax3K and ponticulin-minus mutant cells at comparable developmental stages. In a previous report (Hitt et al., 1994*b*), ponticulin-minus cells were demonstrated to exhibit a shorter preaggregation period than Ax3K cells when developed at low density on agar containing Sorensen's buffer (14.6 mM KH_2PO_4, 2.0 mM Na_2HPO_4, pH 6.0). We found that when cells were plated four deep on development filters saturated with BSS (Fig. 2) or were developed on agar with Sorensen's buffer containing 2.4 mM $MgCl_2$ (data not shown), the preaggregation period and timing of subsequent stages of development were similar for wild-type and mutant cells. In BSS, Ax3K and Tf24.1 cells progressed simultaneously through the ripple (*R*), loose aggregate (*LA*) and tight aggregate (*TA*) stages at 7.0, 8.5, and 9.5 h, respectively (Fig. 2). This latter developmental protocol, therefore, provided the temporal parallelism needed for a valid comparison of behavioral phenotypes, and was used in all studies reported here.

The developmental regulation of motility in both wild-type and mutant cells was also similar through the first 9 h of development under these conditions. In Fig. 2, the mean instantaneous velocity of individual Ax3K and Tf24.1 cells are plotted as functions of developmental time. The mean instantaneous velocity of both cell types was ~2 μm/min during the first 6 h of development , increased to peak values of 9.5 and 11.5 μm/min, respectively, at 7 h of development, and then decreased to 3.5 μm/min at 9 h of development. These results are highly similar to those originally reported for wild-type strain Ax3-clone RC3 (Varnum et al., 1986). Subsequent comparisons of wild-type and ponticulin-minus cells were performed with ripple stage cells removed from filters after 7 h of development (Fig. 2, *R*), at peak instantaneous velocity for all three strains.

Two-Dimensional Motility and Shape Parameters

We initially considered two possible outcomes of a ponticulin-minus phenotype. First, we considered the possibility that a cell lacking ponticulin and, therefore, most of the high affinity linkages between actin and the plasma membrane (Hitt et al., 1994*b*), would translocate at a slower velocity than wild-type cells if the ponticulin-based connections were required for pseudopod extension. Alternatively, we considered it possible that a cell lacking ponticulin might translocate at a faster velocity than wild-type cells if ponticulin–actin connections have to be disrupted for normal pseudopod extension.

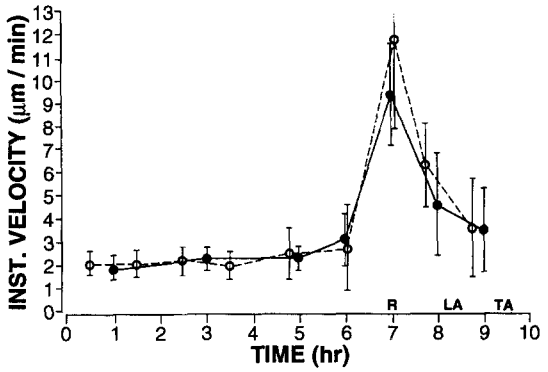

Figure 2. Developmental regulation of single cell motility in wild-type Ax3K and mutant Tf24.1 cultures. Cells were grown to late log phase in nutrient medium and were dispersed on development filters at high cell density in BSS (Soll, 1987). At various time points, developing cultures were disaggregated, single cells were inoculated into a Dvorak-Stotler chamber at low density, and the chamber was perfused with buffer. Cell behavior was video-recorded for 10-min periods at high magnification through DIC optics. The perimeters of 25 randomly selected cells at each time point were digitized into the 2D-DIAS data file at 4-s intervals, and their average instantaneous velocities were computed over the 10-min period of analysis. Each data point represents the mean ± standard deviation of the average instantaneous velocities of the 25 analyzed cells. The developmental stages of Ax3K and Tf24.1 cells were identical in these high-density cultures: *R*, ripple stage (onset of aggregation); *LA*, loose aggregate stage; *TA*, tight aggregate stage. -●-, Ax3K; -○-, Tf24.1.

A 2-D analysis of general motility parameters suggests that ponticulin-minus cells translocate at instantaneous velocities similar to or slightly higher than those of wild-type Ax3K cells (Table I). Both the mean instantaneous velocity and the mean positive flow, a measure of area displacement with time (Soll et al., 1988; Soll, 1988, 1995), were slightly greater for mutant cells than for wild-type cells, although the differences were statistically significant only for Tf1.1 cells vs. wild-type cells (Table I). There were no significant differences in the velocity cycle (Wessels et al., 1994). The mean period between velocity peaks of Ax3K cells was 1.23 ± 0.29 min (n = 24), and that of Tf1.1 and Tf24.1 cells 1.06 ± 0.20 (n = 33) and 1.44 ± 0.75 (n = 21) min, respectively. The differences between mutant and wild-type values were in both cases insignificant ($P > 0.35$). There was also no significant difference between wild-type and mutant cell shape (Table I). Mean maximum length, mean maximum width, mean area, and mean roundness of wild-type and mutant cells were statistically indistinguishable, with values very similar to those previously reported for other wild-type strains of *Dictyostelium* (Wessels et al., 1991; Cox et al., 1992). We, therefore, conclude that ponticulin-minus and wild-type cells crawl in buffer with similar instantaneous velocities, velocity cycles, and general shape.

Table I. Motility and Morphology Measurements of Parental Ax3K and Ponticulin-Minus Transformants (Tf1.1, Tf24.1) Translocating in Buffer

	Mean. Inst. Vel.	Mean Pos. Flow	Mean Max. Len.	Mean Max. Wid.	Mean Area	Mean Round.
	μm/min	*% area*	*μm*	*μm*	*μm²*	*%*
Ax3K (parental) (n = 26)	9.2 ± 2.2	15.9 ± 3.1	19.2 ± 3.8	9.7 ± 1.8	97.9 ± 26.9	43.0 ± 9.8
Tf1.1 (n = 23)	11.1 ± 3.0	19.5 ± 6.4	21.7 ± 4.1	9.6 ± 1.6	105.9 ± 25.7	38.8 ± 9.4
Tf24.1 (n = 13)	10.9 ± 4.4	16.1 ± 5.7	21.5 ± 6.6	9.3 ± 1.0	115.8 ± 38.1	44.7 ± 6.8
P values‡						
Ax3K vs. Tf1.1	0.02	0.02	0.04	NS	NS	NS
Ax3K vs. Tf24.1	NS	NS	NS	NS	NS	NS

*Determinations were made from 2-D cell perimeters manually digitized at 4-s intervals.
*See Materials and Methods for explanations of Parameters. (Mean Inst. Vel.), Mean Instantaneous Velocity; (Mean Pos. Flow), Mean Positive Flow; (Mean Max. Len.), Mean Maximum Length; (Mean Max. Wid.), Mean Maximum Width; Mean Area; Mean Round, (Mean Roundness). All values represent the mean and standard deviation for the number of cells (n) noted.
‡The Student t test was used to assess significance. A P value ≥0.05 was considered not significant.

Formation of Lateral and Anterior Pseudopods

Computer-generated 2-D tracks of the digitized perimeters of ponticulin-minus cells translocating in buffer gave the impression of being slightly wider, on average, than tracks of wild-type cells. Because the width of a perimeter track is affected by the number, shape, and dynamics of lateral pseudopods, and because the majority of lateral pseudopods formed by wild-type cells in buffer are extended off the substratum and are then retracted (Wessels et al., 1994; Soll, 1995), aberrations in the dynamics of lateral pseudopods could affect the width of a perimeter track without significantly affecting instantaneous velocity. To explore the possibility of abnormalities in the shape or position of lateral pseudopods formed by ponticulin-minus cells, we analyzed pseudopod formation in three dimensions (Murray et al., 1992; Wessels et al., 1994, 1996; Soll, 1995).

In dynamic 3-D reconstructions, we observed that wild-type Ax3K cells and ponticulin-minus cells of strain Tf1.1 and Tf24.1 extended lateral pseudopods at comparable frequencies (Table IIA). However, lateral pseudopods formed by Tf1.1 and Tf24.1 cells were significantly more likely to be formed off the substratum than were lateral pseudopods formed by wild-type cells. Only 10–15% of the lateral pseudopods of ponticulin-minus cells were formed on the substratum, i.e., with their ventral surface in contact with the substratum (Table IIA). By contrast, 40% of the lateral pseudopods of wild-type cells were formed on the substratum. This latter proportion is very similar to that previously reported for cells of the wild-type strain Ax3, clone RC3 (Wessels et al., 1994). Therefore, the proportion of lateral pseudopods formed on the substratum by ponticulin-minus cells was approximately three times smaller than that of wild-type cells.

Since lateral pseudopods formed on the substratum have a greater propensity for initiating sharp turns than do lateral pseudopods formed off the substratum (Wessels et al., 1994), one would expect wild-type cells translocating in

Table II. The Proportion of Lateral and Anterior Pseudopods Formed on and off the Substratum by Ax3K, Tf1.1, and Tf24.1 Cells Translocating in Buffer

Strain	No. cells	Pseudopods	Pseudopods	Proportion formed off substratum	Proportion formed on substratum
A. Lateral Pseudopods		*No. lateral*	*Lateral per 5 min.*		
Ax3K	15	93	6.2 ± 2.4	60 ± 23%	40% ± 23
Tf1.1	4	31	7.8 ± 3.6	90 ± 8%	10% ± 8
Tf24.1	5	39	7.8 ± 0.4	85 ± 14%	15% ± 14
P values*					
Ax3K vs Tf1.1			NS	0.02	
Ax3k vs Tf24.1			NS	0.04	
B. Anterior Pseudopods					
		No. anterior	*Anterior per 5 min.*		
Ax3K	6	22	3.8 ± 0.7	40 ± 25%	60% ± 25%
Tf1.1	4	18	4.2 ± 1.1	73 ± 15%	27% ± 15%
Tf24.1	6	25	4.5 ± 1.0	80 ± 12%	22% ± 12%
P values*					
Ax3K vs. Tf1.1			NS	0.02	
Ax3K vs. Tf24.1			NS	0.04	

Determinations were made from dynamic three-dimensional reconstructions generated at 5-s intervals.
*Student t-test was used to assess significance; similar results were obtained with the nonparametric Mann-Whitney test. A P value ≥0.05 was considered not significant.

buffer to turn more often than mutant cells, since a greater proportion of their lateral pseudopods are formed on the substratum. We, therefore, counted the number of sharp turns in centroid tracks which persisted for ≥32 s. The results supported the above prediction. While centroid tracks of Ax3K cells contained turns at a frequency of 0.74 ± 0.20 per min (n = 15), the centroid tracks of ponticulin-minus cells (Tf1.1 and Tf24.1) contained turns at a frequency of 0.45 ± 0.34 (n = 25). The difference was significant, with a $P < 0.01$.

We also examined the proportion of anterior pseudopods formed on and off the substratum. Again, the proportion of anterior pseudopods formed on the substratum by ponticulin-minus cells was only about one-third that observed for wild-type cells (Table IIB). These results suggest that at least some of the defects described above for the more easily characterized lateral pseudopods also are present in anterior pseudopods.

Fates of Lateral Pseudopods

The ultimate fates of lateral pseudopods formed off the substratum differed between wild-type and ponticulin-minus cells. The majority of the lateral pseudopods formed off the substratum by Ax3K cells were retracted back into the main cell body. An example of normal pseudopod retraction by an Ax3K cell is presented in the sequence of wrapped 3-D reconstructions shown in Fig. 3. At 0 s, this cell had no lateral pseudopods, a tapered anterior end which had lifted off the substratum, and a slightly bifurcated uropod. Between 0 and 5 s, the cell extended a lateral pseudopod (*r1*) from the right side of the anterior portion of the main cell body. As is evident in the horizontal view at 5 s (*bottom*), the ventral surface of pseudopod r1 was not in contact with the substratum. Pseudopod r1 was fully extended at 10 s (not shown) and was retracted into the main cell body between 10 and 20 s, as the cell again extended the original anterior pseudopod along the substratum. Since retraction was completed at the main cell body, the uropod retained its original shape. Throughout the process of pseudopod extension and retraction, the ventral surface of pseudopod r1 did not contact the substratum.

Although the majority of lateral pseudopods formed off the substratum by Tf1.1 and Tf24.1 cells also were extended from the anterior portion of the main cell body, significantly fewer completed retraction into the main cell body when compared with wild-type cells. Instead, the majority completed retraction at the uropod. A representative example of this phenomenon is presented in Fig. 4. At 0 s, the beginning of a lateral pseudopod (*r1*) was evident on the right side of this Tf1.1 cell. The horizontal views of the cell (*bottom*) demonstrate that pseudopod r1 was formed off the substratum. Between 0 and 10 s, this pseudopod continued to expand, and a second pseudopod (*l1*) formed on the left side of the cell body, again off the substratum. Between 10 and 15 s, both pseudopods began to retract but they were now positioned at the uropod. By 20 and 30 s, respectively, pseudopods l1 and r1 were com-

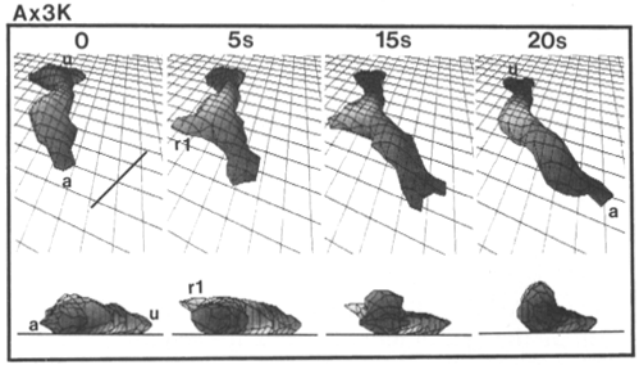

Figure 3. Lateral pseudopods formed off the substratum by Ax3K cells usually complete retraction at the main cell body. (*Top*) 3-D reconstructions of an Ax3K cell viewed from an oblique frontal angle after downward rotation of the anterior end of the 3-D image. (*Bottom*) Horizontal views from the vantage point noted by the black line in the upper panel at time 0. The positions of the anterior end (*a*) and the uropod (*u*) of the cell were determined from the translocation dynamics of the cell before this time series. The cell extended a pseudopod (*r1*) from the right side of the cell body between 0 and 5 s, then retracted it into the cell body between 15 and 20 s. Note in the top panels that the uropod retained its bifurcated shape throughout the time series. In the bottom panels, note that the lateral pseudopod remained off the substratum (i.e., its ventral surface did not make contact with the substratum during extension or retraction).

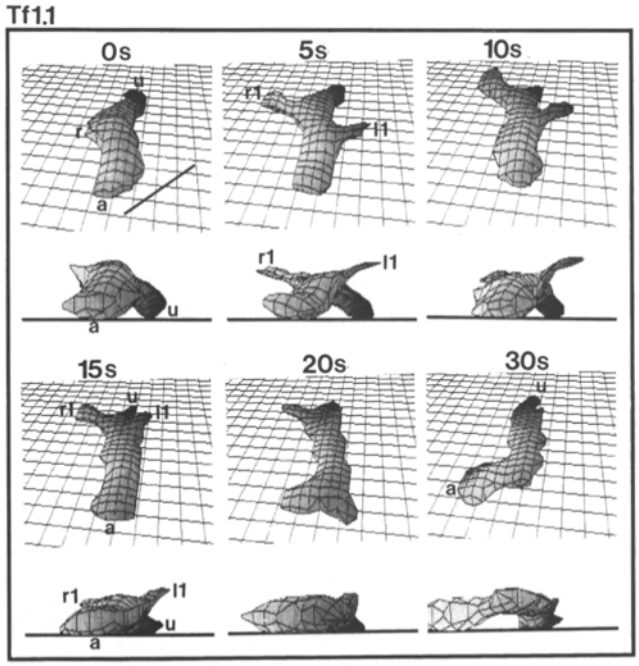

Figure 4. Lateral pseudopods formed off the substratum by ponticulin-minus cells usually complete retraction at the uropod. In the top panel at each time point, the 3-D reconstruction of a Tf1.1 cell is viewed from an oblique frontal angle and in the bottom panel at each time point, the cell is viewed horizontally at the vantage points noted by the black line in the top 0-s panel. The position of the anterior end (*a*) and uropod (*u*) of the cell were determined from the translocation dynamics of the cell prior to the presented time series. This cell extended one pseudopod to the right (*r1*) and one to the left (*l1*) between 0 and 10 sec. Both were formed off the substratum, and both completed retraction at the uropod.

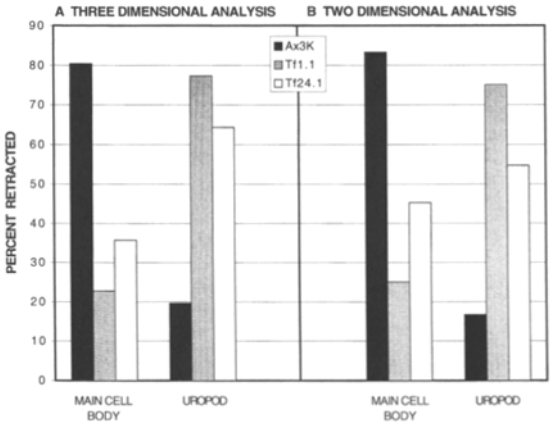

Figure 5. Histograms of the proportions of lateral pseudopods formed off the substratum by wild-type (Ax3K) and mutant (Tf1.1, Tf24.1) cells that were retracted into the main cell body or absorbed into the uropod. (*A*) A 3-D analysis of 20 Ax3K, 28 Tf1.1, and 33 Tf24.1 pseudopods. (*B*) A 2-D analysis of 58 Ax3K, 59 Tf1.1, and 63 Tf24.1 pseudopods. Means and standard deviations for the proportion of retracted pseudopods completing retractions at the main cell body for Ax3K, Tf1.1, and Tf24.1 cells in the 3-D study were 81 ± 24, 23 ± 19, and 36 ± 17%, and at the uropod 19 ± 24, 77 ± 19, and 64 ± 17%. Means and standard deviations for the proportion completing retraction at the main cell body for Ax3K, Tf1.1, and Tf24.1 in the 3-D study were 83 ± 14, 25 ± 15, and 45 ± 21%, and at the uropod 17 ± 14, 75 ± 15, and 55 ±21%. The differences in the proportions of pseudopods retracted into the main cell body between Ax3K and Tf1.1 and between Ax3K and Tf24.1 were statistically significant, with *P* values <0.05.

pletely absorbed. The uropod, in this case, changed its shape as a consequence of absorption. Such shape changes were always observed concommitant with absorption at the uropod, suggesting that they are diagnostic for this phenomenon.

The difference between wild-type and mutant cells in the position along the cell body at which pseudopod retraction is completed was quantified using 3-D (Fig. 5 *A*) and 2-D (Fig. 5 *B*) analyses. In both cases, ≥80% of the lateral pseudopods formed off the substratum by wild-type Ax3K cells were retracted into main cell body. In marked contrast, up to 75% of the pseudopods extended off the substratum by ponticulin-minus cells completed retraction at the uropod.

Pseudopods of Ponticulin-Minus Cells Slip Posteriorly

One explanation for the positional difference in lateral pseudopod retraction (Fig. 5) is that pseudopods in ponticulin-minus cells may exhibit a longer average lifespan due to a decrease in the rate of pseudopod extension and/or retraction. For a cell rapidly translocating in buffer, a longer-lived lateral pseudopod would be more likely to remain extended as the cell translocated anteriorly, and the consequence would be completion of retraction at the uropod. To test this possibility, we analyzed the rates and periods of expansion and retraction of lateral pseudopods (Table III). The results showed no significant differences between Ax3K and ponticulin-minus cells in the rate of expansion, the rate of retraction, or the longevity of lateral pseudopods formed off the substratum.

Table III. Rates of Expansion and Contraction of Lateral Pseudopods Formed off the Substratum in Wild-type and Ponticulin-Minus Cells

Strain	No. Pseudopods	Avg. Rate of Expansion	Expansion Period	Avg. Rate of Retraction	Retraction Period
		$\mu m^3/5$ s	s	$\mu m^3/5$ s	s
Ax3K	15	15 ± 10	29 ± 22	8 ± 5	45 ± 27
Tf1.1 + Tf24.1	15	11 ± 18	34 ± 20	5 ± 4	39 ± 16
P value*		NS	NS	NS	NS

Measurements are based on a 3-D analysis.
*Student *t*-test was used to assess significance. A *P* value ≥0.05 was considered not significant.

Another explanation for the positional difference in lateral pseudopod retraction (Fig. 5) is that the lateral pseudopods of ponticulin-minus cells may be positionally unstable, (i.e., more inclined to slip posteriorly relative to the cell body and/or the substratum), and, therefore, more likely to complete retraction at the uropod. In wild-type cells, we discovered that the position of every lateral pseudopod formed off the substratum remained fixed in relation to the substratum through the entire extension and retraction process, even during translocation of the cell (Fig. 6; Table IV). This positional invariance was observed both for the majority of lateral pseudopods, which were retracted into the main cell body (Fig. 6 *A*, *r2*), and for the majority of lateral pseudopods, which completed retraction at the uropod (Fig. 6 *A*, *r1*). Positional invariance of each lateral pseudopod formed off the substratum was observed not only for the Ax3K parental strain in this study, but also for strain Ax3, clone RC3 (Table IV, Fig. 6 *B*), and strain Ax2 (Table IV), two other laboratory strains of *Dictyostelium discoideum* that have been used in previous computer-assisted analyses of cell motility (Wessels et al., 1989, 1992, 1994). Of 104 lateral pseudopods formed by 14 wild-type axenic cells, 100% remained fixed in relation to the substratum, i.e., none showed positional slippage (Table IV).

In marked contrast, lateral pseudopods formed off the substratum by ponticulin-minus cells were not positionally fixed relative to the substratum (Fig. 7; Table IV). Half or more of these lateral pseudopods changed positions in relation to the substratum during expansion and retraction (Table IV). Most of these unfixed pseudopods slipped posteriorly; none were observed to slip towards the front of the cell. In the case of pseudopod r1, formed by the representative Tf1.1 cell in Fig. 7, the distance that the base of the pseudopod slipped in relation to the substratum (noted by a dotted line at 10 s) was 6.25 μm, which represents a minimum retrograde velocity of 75 μm/min. Pseudopod l1 on this same cell slipped 5 μm in the same 5-s period and an additional 5 μm in the next 5-s period, which represents a minimum retrograde velocity of 60 μm/min. Of 76 lateral pseudopods formed by 11 ponticulin-minus cells, over half slipped and in all cases they did so in the posterior direction (Table IV). Every mutant cell analyzed for a period of 3–10 min exhibited slippage of one or more pseudopods (Table IV).

Pseudopod slippage in ponticulin-minus cells also occurred in the z-axis (Fig. 8). In some cases, lateral pseudopods that were formed off the substratum by ponticulin-

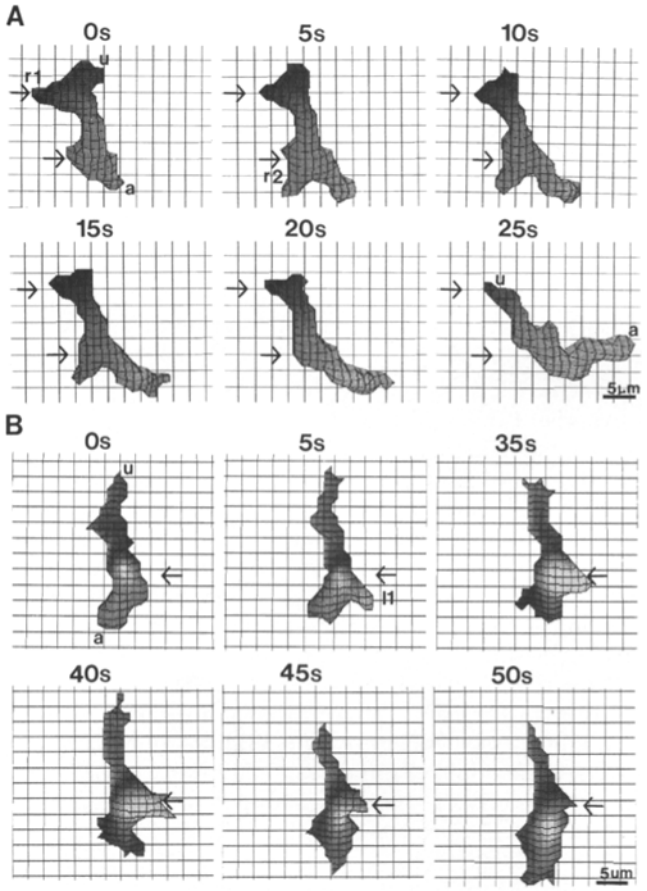

Figure 6. The base of each lateral pseudopod formed by wild-type cells remains fixed relative to the substratum during both extension and retraction. (*A*) A representative Ax3K cell; (*B*) A representative Ax3-clone RC3 cell. The reconstructions are viewed dorsally so that the position of the base of each pseudopod can be established and marked by an arrow on the underlying grid. The positions of the anterior end (*a*) and uropod (*u*) of the cell at 0 s of each time sequence were determined from the translocation dynamics of the cell before the presented time series. The Ax3K cell in *A* had already formed a lateral pseudopod to its right (*r1*) before 0 s and another to its right (*r2*) between 0 and 5 s. The Ax3-RC3 cell in *B* formed a lateral pseudopod to its left (*l1*) between 0 and 5 s.

minus cells appeared to be absorbed into the main cell body when viewed dorsally (Fig. 8, *top*). However, when the same cells were viewed from a horizontal vantage point, it was clear that the pseudopod had rotated to the dorsal surface of the cell and then slipped posteriorly to the uropod (Fig. 8, *bottom*). Thus, the top views of the representative Tf24.1 cell in Fig. 8 failed to discriminate between pseudopod retraction and circumferential slippage to the dorsal surface of the cell body. In the case of the cell in Fig. 8, the pseudopod on the dorsal surface of the cell slipped 7.5 μm toward the posterior end of the cell (Fig. 8, *dotted line*) between 15 and 25 s, which represents a retrograde velocity of 45 μm/min. At 25 s, this dorsal pseudopod was positioned at the uropod. Since the proportion of pseudopods which slipped posteriorly (Table IV) was determined from 2-D reconstructions in which dorsal slippage such as that demonstrated in Fig. 7 would not have been detected, the reported proportions of slippage by lateral pseudopods of Tf1.1 and Tf24.1 cells in Table IV are probably underestimates.

Table IV. Lateral Pseudopod Slippage in Ponticulin-Minus (Tf1.1, Tf24.1) Cells

Strain	No. cells	No. lateral pseudopods	Percentage pseudopod slippage	Percentage cells exhibiting slippage*
Ax3K	5	53	0	0
Ax3(RC3)	4	26	0	0
Ax2	5	25	0	0
Tf1.1	6	47	49	100
Tf24.1	5	29	55	100

The relationship of the base of each pseudopod to the substratum was determined during extension and retraction from 2-D perimeters hand-digitized at 4-s intervals.
*The proportion of cells exhibiting at least one case of lateral pseudopod slippage during the period of analysis, which was between 3 and 10 min per cell.

Chemotactic Inefficiency of Ponticulin-Minus Cells

Lateral pseudopods that are extended off the substratum have been suggested to play a key role in sensing chemotactic gradients (Varnum-Finney et al., 1987*b*; Wessels et al., 1994; Soll, 1995) and in initiating turns in the correct direction (i.e., in the direction of increasing cAMP concentration). Thus, cells with lateral pseudopods that frequently slip posteriorly and/or dorsally might be expected to be less efficient in tracking a spatial gradient (see Discussion).

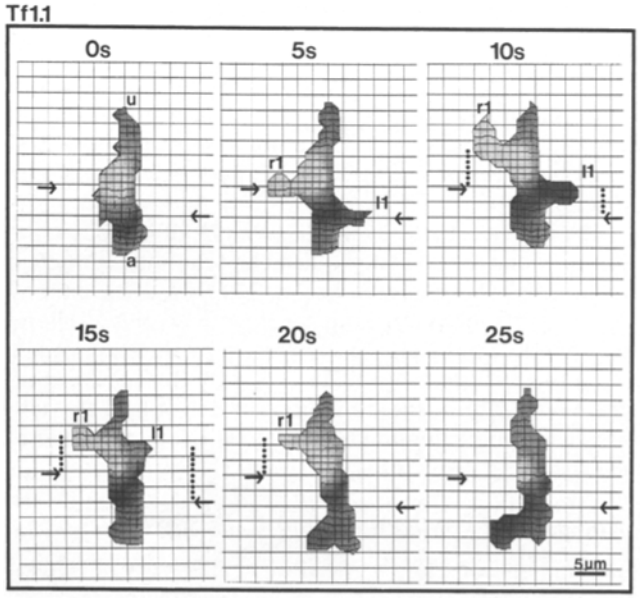

Figure 7. Lateral pseudopods formed by ponticulin-minus cells are not anchored to the substratum and slip posteriorly. The anterior end (*a*) and uropod (*u*) of this representative Tf1.1 cell were determined from the translocation dynamics before the presented time series. The reconstructions are viewed dorsally. Arrows denote the original position of the base of each pseudopod in relation to the substratum on the underlying grid. This representative Tf1.1 cell formed one pseudopod to the right (*r1*) and one pseudopod to the left (*l1*) between 0 and 5 s. Both pseudopods then slipped posteriorly, and the distances that they slipped are noted by dotted lines. This figure represents the same cell and time series viewed from oblique and horizontal angles in Fig. 3, which showed that neither r1 nor l1 contacted the substratum.

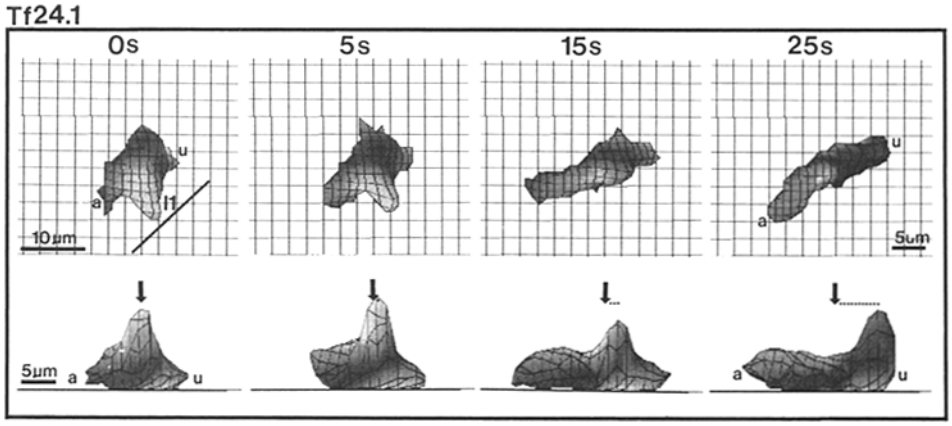

Figure 8. In some cases, lateral pseudopods formed off the substratum by ponticulin-minus cells rotate to the dorsal surface of the cells as they slip posteriorly. In the top panel at each time point, the reconstruction of the representative Tf24.1 cell is viewed dorsally, and in the bottom panel at each time point, the cell is viewed horizontally from the vantage point noted by the black line in the top panel at 0 s. This particular ponticulin-minus cell had formed a pseudopod to its left (*l1*) before 0 s. In the dorsal views, this pseudopod appeared to be retracted between 5 and 15 s; in the horizontal views, it is clear that the pseudopod first slipped circumferentially to the dorsal surface of the cell and then slipped posteriorly. *Black arrow*, the original position of the pseudopod in relation to the substratum. *Dotted lines*, the distance it slips in relation to the substratum.

The mean CI of ponticulin-minus cells was significantly less than that of wild-type cells (Fig. 9). The mean CI for Ax3K cells was $+0.45 \pm 0.29$ ($n = 66$), while that for Tf1.1 was $+0.30 \pm 0.29$ ($n = 48$) and that for Tf24.1 was $+0.30 \pm 0.30$ ($n = 52$). The difference between the mean CIs of Ax3K and Tf1.1 cells, and the CIs of Ax3K and Tf24.1 cells were highly significant. In the former case, the P value was 0.006 and in the latter case 0.007. In contrast, the P value for the mean CIs of Tf1.1 and Tf24.1 was 0.986, demonstrating an extremely high similarity between the two mutant strains. The difference in the distributions of CIs of wild-type and mutant cells is demonstrated in the histogram in Fig. 9, in which the pooled data for the two mutants is compared with that of wild-type cells. Perhaps even more important than the shift in the average CI is the dramatic decrease in the proportion of mutant cells that achieve high end CIs. While 33% of wild-type cells exhibited CIs of 0.6–0.8, only 17% of mutant cells did so, and while 8% of wild-type cells exhibited CIs of 0.8–1.0, no mutant cells were this efficient.

The decrease in the chemotactic efficiency of ponticulin-minus cells appears to be due to an increase in the frequency of sharp turns away from the direction of the gradient (i.e., away from the direction of increasing concentration of chemoattractant). In Fig. 10, *A* and *B*, the perimeter and centroid tracks of a wild-type cell and a ponticulin-minus cell with comparable instantaneous velocities and very high CIs are compared. Although both cells were moving up the spatial gradient, the mutant cell made two small lateral deviations that lowered its chemotactic index. In each case, the deviation was due to a mistaken turn (i.e., a turn away from the direction of the source) generated by extension of a lateral pseudopod. These deviations generated kinks in the centroid track (Fig. 10 *B*). An examination of the tracks of the 10 Ax3K and 10 ponticulin-minus cells with the highest CIs demonstrated that mutant cells, on average, made more lateral turning mistakes. In Fig. 9, *C* and *D*, perimeter and centroid tracks are presented for a wild-type cell and ponticulin-minus cell with similar instantaneous velocities and CIs close to the median. Again, the net direction of migration of the wild-type and the mutant cell is in the direction of the source of chemoattractant, but the mutant cell made more turning mistakes than the wild-type cell. An examination of the 10 Ax3K and 10 ponticulin-minus cells with CIs closest to the mean of each group demonstrated that mutant cells, on average, made more lateral turning mistakes.

Discussion

We demonstrate here that lateral pseudopods formed off the substratum by wild-type *Dictyostelium* amoebae translocating in buffer remain fixed in relation to the substratum as they are extended and retracted, even though the main cell body may continue to translocate anteriorly. Because the ventral surfaces of lateral pseudopods formed off the substratum are not in contact with the substratum,

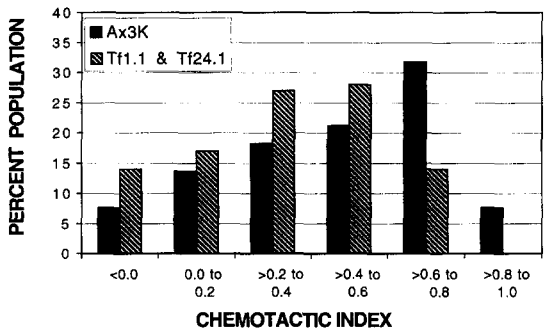

Figure 9. The high end of chemotactic indices is underrepresented in ponticulin-minus cells chemotaxing in a spatial gradient of the chemoattractant, cAMP. Ax3K (*filled bars*) and ponticulin-minus cells (*hatched bars*) were distributed on the bridge of a gradient chamber bordered by a trough filled with buffer only and a trough filled with buffer plus 1 μM cAMP. After 4 min, cellular behavior was recorded, and the CI of each cell was computed according to the formula described in Materials and Methods. Data were pooled from six separate experiments with Ax3K cells and from four separate experiments with each of the ponticulin-minus cell lines. The mean CI ± SD and the number of analyzed cells for Ax3K and the pooled mutant cells were 0.45 ± 0.29 ($n = 66$) and 0.30 ± 0.29 ($n = 100$), respectively. The difference between the means is highly significant ($P < 0.01$) determined both by the T test and the Mann-Whitney nonparametric test.

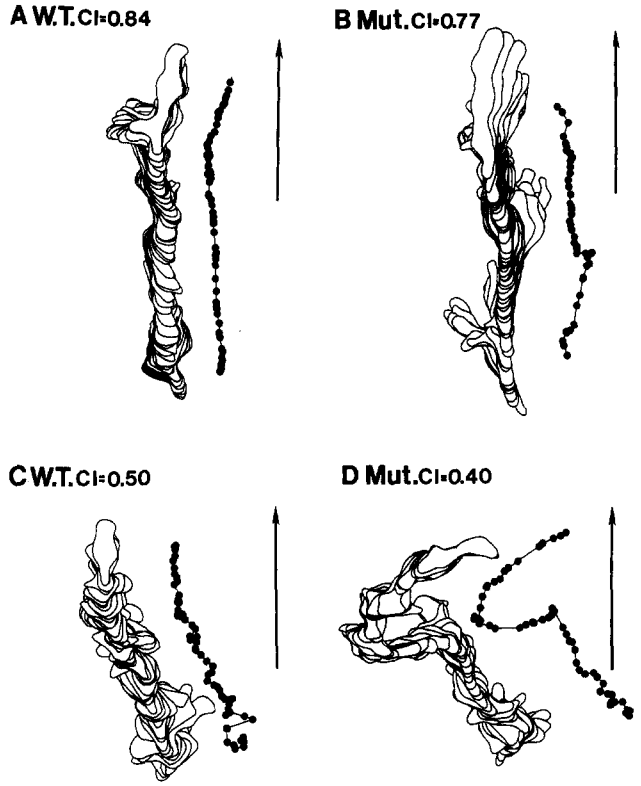

Figure 10. Perimeter and centroid plots of a wild-type cell (*A*) and a ponticulin-minus cell (*B*) with comparable instantaneous velocities and very high chemotactic indices (*CI*), and of a wild-type cell (*C*) and a ponticulin-minus cell (*D*) with comparable instantaneous velocities and CIs close to the median.

these pseudopods must be anchored to the substratum through interactions between the substratum and cortical and/or plasma membrane proteins in that portion of the cell body from which the pseudopod extends. Presumably, these interactions involve actin-based supramolecular cytoskeletal structures that connect the substratum with the plasma membrane, the cortex of the cell body and the cortex of the pseudopod.

We also have demonstrated here that ponticulin, a transmembrane protein responsible for most of the high affinity binding between F-actin and the *Dictyostelium* plasma membrane (Wuestehube and Luna, 1987; Wuestehube et al., 1989; Chia et al., 1991; Hitt et al., 1994*a*,*b*), is required for positionally fixing lateral pseudopods relative to the substratum, since the lateral pseudopods formed off the substratum by these mutant cells undergo frequent and dramatic slippage. Slippage can occur during both extension and retraction, and occurs primarily in the posterior direction. Pseudopods can also slip circumferentially to the top of a cell, and then slip posteriorly. Such circumferential slippage may be responsible for the significant increase in the proportion of both lateral and anterior pseudopods formed off the substratum by ponticulin-minus cells, since pseudopods that slip dorsally have less chance of contacting and subsequently extending along the substratum (Wessels et al., 1994).

This basic behavioral defect of ponticulin-minus cells is quite specific to this mutant. Ponticulin-minus cells translocating in buffer still extend pseudopods with the same frequency and growth dynamics as wild-type cells, and retract pseudopods with the same dynamics as wild-type cells. They exhibit the same periodicity in their velocity cycle as wild-type cells and can readily sense a gradient of chemoattractant, although with less efficiency. Their basic behavioral defect is, specifically, the loss of the positional stabilization of lateral pseudopods in relation to the substratum and subsequent pseudopod slippage. This mutant phenotype leads to a number of additional behavioral defects and contrasts markedly with that of myosin IA and B mutants, which are defective primarily in the frequency of pseudopods formed on the substratum (Wessels et al., 1991, 1996; Titus et al., 1993). It also contrasts with that of ABP-120 mutants, which are defective in the frequency of pseudopod formation and the rate and extent of pseudopod expansion (Cox et al., 1992; Cox, D., D. Wessels, D. R. Soll, J. Hartwig, and J. Condeelis, manuscript submitted for publication), with that of myoII mutants, which are defective in polarity, the original position of pseudopod extension, and the rate and extent of pseudopod growth (Wessels et al., 1988; Wessels and Soll, 1990), and with that of the discoidinless mutants, which are capable of rapid translocation in spite of their aberrant blunt morphology and loss of a conventional tapered uropod (Alexander et al., 1992).

Pseudopod slippage in ponticulin-minus cells correlates with a number of behavioral defects for cells translocating in buffer and for cells chemotaxing in a spatial gradient of cAMP. All of these defects may be consequences of slippage. First, ponticulin-minus cells translocating in buffer complete the process of pseudopod retraction at a more posterior cellular position than wild-type cells. In wild-type cells, most lateral pseudopods formed off the substratum extend from the anterior portion of the main cell body and are retracted primarily into the middle or posterior portion of the main cell body, just anterior to the uropod. This appears to be a consequence of the forward movement of the cell and the fixed position of the pseudopod in relation to the substratum. In wild-type cells, the morphological integrity of the uropod is, therefore, maintained throughout the 3-D behavior cycle of most cells (Wessels et al., 1994; Soll, 1995). In marked contrast, most pseudopods formed off the substratum by ponticulin-minus cells complete the retraction process at the uropod, with an accompanying characteristic alteration of uropod morphology. Pseudopod slippage obviously accounts for posteriorization of the retraction process in these mutants.

Ponticulin-minus cells translocating in buffer also exhibit altered turning behavior. Pseudopods formed by wild-type cells off the substratum have a greater propensity for being retracted and are less likely to initiate a sharp turn than pseudopods formed on the substratum (Wessels et al., 1994). Ponticulin-minus cells form a far greater proportion of their pseudopods off the substratum, which most likely explains why they translocate in buffer with a lower frequency of turning.

Finally, ponticulin-minus cells exhibit a decrease in the efficiency of chemotaxis. This decrease is due to an increase in turning mistakes made by ponticulin-minus cells moving up a spatial gradient of the chemoattractant cAMP. Superficially, this observation appears to contradict the observa-

tions made on turning in buffer, namely that slippage leads to a decrease in turning. However, inappropriate pseudopod slippage would be expected to lead to a depression in chemotactic efficiency since there is strong reason to believe that the spatial stability of lateral pseudopods is necessary for sensing a spatial gradient of chemoattractant and reorienting (Varnum-Finney et al., 1987*b*; Soll et al., 1993; Soll, 1995). Cells moving towards the source of a spatial gradient form lateral pseudopods at roughly one-third the frequency of cells moving in buffer, and the fewer lateral pseudopods which do form generate turns at a lower frequency (Varnum-Finney et al., 1987*b*), suggesting that they are formed primarily off the substratum and, therefore, have a greater propensity for being retracted. In addition, cells oriented at an angle towards the source of chemoattractant form as many lateral pseudopods towards as away from the source, but turn into the former two to three times as frequently as they do into the latter (Varnum-Finney et al., 1987*b*). These results suggest that lateral pseudopods formed by cells in a spatial gradient sense the direction of the gradient and either fall to the substratum to initiate a turn when sensing a positive gradient or remain off the substratum and are retracted when sensing a negative gradient (Soll, 1995). Within this context, the loss of the positional stability of pseudopods by ponticulin-minus cells would diminish the efficiency of chemotaxis by three possible mechanisms. First, if a lateral pseudopod rotates to the dorsal surface of a cell, it would be perpendicular to the gradient of chemoattractant and, therefore, incapable of sensing it. This outcome would depress the average chemotactic index because cells veering off track would produce fewer compensating sharp turns (Soll et al., 1993). Second, if a lateral pseudopod slipped posteriorly along the cell axis, it would also move through the gradient in a direction of decreasing concentration, which would confuse a temporal and/or spatial mechanism of gradient assessment (Soll et al., 1993; Soll, 1995). Again, this outcome would depress the average chemotactic index by decreasing the efficiency of reorientation. Third, if a lateral pseudopod slipped to the substratum during sensing, it would initiate an inappropriate turn, and result in a depression in chemotactic index. It is likely that all three outcomes contribute to the decrease in chemotactic efficiency observed in ponticulin-minus cells.

Therefore, the loss of the positional stability of pseudopods and the corresponding decrease in chemotactic efficiency of ponticulin-minus cells suggests that ponticulin is involved in at least one step in the chemotactic signal–response pathway of *Dictyostelium*. One intriguing possibility is that ponticulin is involved in stabilizing a sensing pseudopod as it extends through a spatial gradient of attractant off the substratum, and that a pseudopod which senses an increasing concentration of attractant (i.e., is extending up a concentration gradient towards the source of attractant) falls to the substratum to initiate a turn by destabilizing the pseudopod through the regulation of ponticulin.

Posterior slippage of lateral pseudopods along the long axis of cells shares some morphological similarities to the capping of cell surface receptors. However, these two phenomena occur at dramatically different velocities. Lateral pseudopods formed by ponticulin-minus mutants slip posteriorly at ~50–60 μm/min, which is about an order of magnitude faster than the velocity with which *Dictyostelium* amoebae cap beads coated with lectin (Pasternak et al., 1989; Jay and Elson, 1992). The velocity of lateral pseudopod slippage is also at least five times faster than the mean instantaneous velocity of cellular translocation. The velocity of pseudopod slippage is, however, comparable to the instantaneous velocities of intracellular particles moving within the central cytoplasm of rapidly translocating wild-type *Dictyostelium* amoebae (Wessels and Soll, 1990), but these particles were observed to move primarily towards the front of the cell. Since the velocity of these forward moving particles was roughly five times that of cellular translocation, there would either have to be dissolution of the particles at the anterior edge of the particulate cytoplasm or a retrograde compensatory current of particles, perhaps in the cytoplasmic cortex, to account for the fact that particles do not accumulate in the front of a cell. The absence of posterior slippage of lateral pseudopods in wild-type cells suggests that ponticulin is integral to a plasma membrane–associated cytoskeletal structure that normally resists the suggested rearward flow of cortical cytoplasm. Posterior pseudopod slippage in ponticulin-minus cells is consistent with the contraction-hydraulic (Mast, 1926; Jahn, 1964) and cortical flow (Bray and White, 1988) models of cellular translocation, in which fountains of submembranous cytoplasm (Grebecki, 1994) move rearward in regions of the cell not attached to the substratum.

The absence of posterior pseudopod slippage in wild-type cells suggests that ponticulin is involved in a plasma membrane–associated cytoskeletal structure (membrane skeleton) that normally resists the putative rearward flow of cytoplasm. Ponticulin-based anchorage of lateral pseudopods relative to the substratum is consistent with the general role played by membrane skeleton proteins in separating regions of the plasma membrane into discrete functional domains (for review see Luna and Hitt, 1992). Another implication of our results is that pseudopods, although dynamic in nature, may be thought of as plasma membrane domains that are stabilized and regulated by membrane skeleton proteins, such as ponticulin. In conjunction with other recently described regions of membrane specialization in motile cells (for review see Sheetz, 1995), our observations suggest that the membrane skeletons of motile cells are at least as complex as, though much less well understood than, the membrane skeletons of more static cells such as erythrocytes and epithelial cells.

Because the formation of pseudopods on and off the substratum and the periodicity of the motility cycle of *Dictyostelium* amoebae translocating in buffer are strikingly similar to several behavioral aspects of polymorphonuclear leukocytes (Murray et al., 1992) and of T cells and giant HIV-induced T cell syncytia (Sylwester et al., 1993, 1995), a final implication of our results is that precise temporal and spatial regulation of pseudopod dynamics may be a general requirement for the taxis of many chemotactically responsive mammalian cells. Therefore, proteins with structural and functional similarities to *Dictyostelium* ponticulin may play critical roles in morphogenesis, the cellular immune system, and other biological processes in which amoeboid cells must move in a directed fashion through extension of actin-based pseudopods.

The authors are indebted to Dr. Edward Voss for helping run the 3D-DIAS program and for computing 3D-DIAS errors, and to Jim Trepka for developing the precision stepper motor for optical sectioning.

This research was supported in part by grant HD 18577 from the National Institutes of Health (NIH) to D. R. Soll, by a grant from the Iowa Economic Development Commission to D. R. Soll to develop 3D-DIAS, by a grant from Wallace Technologies to D. R. Soll to develop the microstepper motor, and by grant GM33048 from NIH to E. J. Luna.

Received for publication 4 May 1995 and in revised form 29 September 1995.

References

Abercrombie, M., J. E. M. Heaysman, and S. M. Pegrum. 1970*a*. The locomotion of fibroblasts in culture. I. Movements of the leading edge. *Exp. Cell Res.* 59:393–398.

Abercrombie, M., J. E. M. Heasyman, and S. M. Pegrum. 1970*b*. The locomotion of fibroblasts in culture. II. Ruffling. *Exp. Cell Res.* 60:437–444.

Alexander, S., L. Sydow, D. Wessels, and D. R. Soll. 1992. *Discoidin* proteins of *Dictyostelium* are necessary for normal cytoskeletal organization and cellular morphology during translocation. *Differentiation.* 51:149–161.

Bray, D., and J. G. White. 1988. Cortical flow in animal cells. *Science (Wash. DC).* 239:883–888.

Caterina, M. J., and P. N. Devreotes. 1991. Molecular insights into eukaryotic chemotaxis. *FASEB J.* 5:3078–3085.

Chandrasekhar, A., D. Wessels, and D. R. Soll. 1995. A mutation that abolishes cGMP phosphodiesterase activity in *Dictyostelium* selectively affects cell behavior in the back of the chemotactic wave. *Dev. Biol.* 169:109–122.

Chia, C. P., A. L. Hitt, and E. J. Luna. 1991. Direct binding of F-actin to ponticulin, an integral plasma membrane glycoprotein. *Cell Motil. Cytoskeleton.* 18:164–179.

Cocucci, S., and M. Sussman. 1970. RNA in cytoplasmic and nuclear fractions of cellular slime mold amebae. *J. Cell Biol.* 45:399–407.

Condeelis, J. 1993. Life at the leading edge: the formation of cell protrusions. *Annu. Rev. Cell Biol.* 9:411–444.

Condeelis, J., J. Jones, and J. E. Segall. 1992. Chemotaxis of metastatic tumor cell. Clues to mechanisms from the *Dictyostelium* paradigm. *Cancer Metastasis Rev.* 11:55–68.

Cox, D., J. Condeelis, D. Wessels, D. R. Soll, H. Kern, and D. A. Knecht. 1992. Targeted disruption of the ABP-120 gene leads to cells with altered motility. *J. Cell Biol.* 116:943–955.

DeLozanne, A., and J. A. Spudich. 1987. Disruption of the *Dictyostelium* myosin heavy chain gene by homologous recombination. *Science (Wash. DC).* 236:1086–1091.

Doolittle, K. W., I. Reddy, and J. G. McNally. 1995. 3D analysis of cell movement during normal and mysoin II null cell morphogenesis in *Dictyostelium. Dev. Biol.* 167:118–129.

Downey, G. P. 1994. Mechanisms of leukocyte motility and chemotaxis. *Curr. Opin. Immunol.* 6:113–124.

Grebecki, A. 1994. Membrane and cytoskeleton flow in motile cells with emphasis on the contribution of free-living amoebae. *Int. Rev. Cytol.* 148:37–80.

Hitt, A. L, T. H. Lu, and E. J. Luna. 1994*a*. Ponticulin is an atypical membrane protein. *J. Cell Biol.* 126:1421–1431.

Hitt, A. L., J. H. Hartwig, and E. J. Luna. 1994*b*. Ponticulin is the major high affinity link between the plasma membrane and the cortical actin network in *Dictyostelium. J. Cell Biol.* 126:1433–1444.

Jahn, T. L. 1964. Relative motion in *Amoeba proteus. In* Primitive Motile Systems in Cell Biology. R. D. Allen and N. Kamiya, editors. Academic Press, Inc. New York. 279–302.

Jay, P. J., and E. L. Elson. 1992. Surface particle transport mechanism independent of myosin II in *Dictyostelium. Nature (Lond.).* 356:438–440.

Knecht, D. A., and W. F. Loomis. 1987. Antisense RNA inactivation of myosin heavy chain gene expression in *Dictyostelium discoideum. Science (Wash. DC).* 236:1081–1086.

Luna, E. J, and A. L. Hitt. 1992. Cytoskeleton-plasma membrane interactions. *Science (Wash. DC).* 258:955–964.

Luna, E. J., L. J. Wuestehube, C. P. Chia, A. Shariff, A. L. Hitt, and H. M. Ingalls. 1990. Ponticulin, a developmentally-regulated plasma membrane glycoprotein, mediates actin binding and nucleation. *Dev. Genet.* 11:354–361.

Mast, S. O. 1926. Structure, movement, locomotion and stimulation in *Amoeba. J. Morphol. Physiol.* 41:347–425.

McCutcheon, M. 1946. Chemotaxis in leukocytes. *Physiol. Rev.* 26:401–404.

Murray, J., H. Vawter-Hugart, E. Voss, and D. R. Soll. 1992. A three-dimensional motility cycle in leukocytes. *Cell Motil. Cytoskeleton.* 22:211–223.

Pasternak, C., J. A. Spudich, and E. L. Elson. 1989. Capping of surface receptors and concomitant cortical tension are generated by conventional myosin. *Nature (Lond.).* 341:549–551.

Schindl, M., E. Wallraff, B. Deubzer, W. Witke, G. Gerisch, and E. Sackman. 1995. Cell substrate interactions and locomotion of *Dictyostelium* wild-type and mutants defective in three cytoskeletal proteins: a study using quantitative reflection interference contrast microscopy. *Biophys. J.* 68:1177–1190.

Shariff, A., and E. J. Luna. 1990. *Dictyostelium discoideum* plasma membranes contain an actin-nucleating activity that requires ponticulin, an integral membrane glycoprotein. *J. Cell Biol.* 110:681–692.

Sheetz, M. 1995. Cellular plasma membrane domains. *Mol. Membr. Biol.* 12:89–91.

Sheldon, E., and D. A. Knecht. 1995. Mutants lacking myosin II cannot resist forces generated during multicellular morphogenesis. *J. Cell Sci.* In press.

Soll, D. R. 1979. Timers in developing systems. *Science (Wash. DC).* 203:841–849.

Soll, D. R. 1987. Methods for manipulating and investigating developmental timing in *Dictyostelium discoideum. In* Methods of Cell Biology. Vol. 28. J. Spudich, editor. Academic Press, Inc. San Diego, CA. 413–431.

Soll, D. R. 1988. "DMS," a computer-assisted system for quantitating motility, the dynamics of cytoplasmic flow and pseudopod formation: its application to *Dictyostelium* chemotaxis. *Cell Motil. Cytoskeleton.* 10:91–106.

Soll, D. R., E. Voss, B. Varnum-Finney, and D. Wessels. 1988. The "dynamic morphology system": a method of quantitating changes in shape, pseudopod formation and motion in normal mutant amebae of *Dictyostelium discoideum. J. Cell. Biochem.* 37:177–192.

Soll, D. R., D. Wessels, and A. Sylwester. 1993. The motile behavior of amoebae in the aggregation wave in *Dictyostelium discoideum. In* Experimental and Theoretical Advances in Biological Pattern Formation. H. G. Othmer, P. K. Maini, and J. D. Murray, editors. Plenum Publishing Corp. New York. 325–338.

Soll, D. R. 1995. The use of computers in understanding how cells crawl. *Int. Rev. Cytol.* In press.

Sussman, M. 1987. Cultivation and synchronous morphogenesis of *Dictyostelium* under controlled experimental conditions. *In* Methods in Cell Biology. Vol. 28. J. Spudich, editor. Academic Press, Inc. San Diego, CA. 413–431.

Sylwester, A., D. Wessels, S. A. Anderson, R. Q. Warren, D. Shutt, R. Kennedy, and D. R. Soll. 1993. HIV-induced syncytia of a T cell line form a single giant pseudopod and are motile. *J. Cell Sci.* 106:941–953.

Sylwester, A., D. Shutt, D. Wessels, J. T. Stapleton, J. Stites, R. Kennedy, and D. R. Soll. 1995. T cells and HIV-induced T cell syncytia exhibit the same velocity when translocating on plastic, collagen or endothelial monolayers. *J. Leukocyte Biol.* 57:643–650.

Titus, M. A., D. Wessels, J. A. Spudich, and D. R. Soll. 1993. The unconventional myosin encoded by the *myo*A gene plays a role in *Dictyostelium* motility. *Mol. Biol. Cell.* 4:233–246.

Varnum, B., and D. R. Soll. 1984. Effects of cAMP on single cell motility in *Dictyostelium. J. Cell Biol.* 99:1151–1155.

Varnum, B., K. Edwards, and D. R. Soll. 1986. The developmental regulation of single cell motility in *Dictyostelium discoideum. Dev. Biol.* 113:218–227.

Varnum-Finney, B., E. Voss, and D. R. Soll. 1987*a*. Amebae of *Dictyostelium discoideum* respond to an increasing temporal gradient of the chemoattractant cAMP with a reduced frequency of turning: evidence for a temporal mechanism in ameboid chemotaxis. *Cell Motil. Cytoskeleton.* 8:7–17.

Varnum-Finney, B., E. Voss, and D. R. Soll. 1987*b*. Frequency and orientation of pseudopod formation of *Dictystelium discoideum* amebae chemotaxing in spatial gradient: further evidence for a temporal mechanism. *Cell Motil. Cytoskeleton.* 8:18–26.

Wessels, D., and D. R. Soll. 1990. Myosin II heavy chain null mutant of *Dictyostelium* exhibits defective intracellular particle movement. *J. Cell Biol.* 111: 1137–1148.

Wessels, D., D. R. Soll, D. Knecht, W. F. Loomis, D. DeLozanne, and J. Spudich. 1988. Cell motility and chemotaxis in *Dictyostelium* amebae lacking myosin heavy chain. *Dev. Biol.* 128:164–177.

Wessels, D., N. Schroeder, E. Voss, A. L. Hall, J. Condeelis, and D. R. Soll. 1989. cAMP-mediated inhibition of intracellular particle movement and actin reorganization in *Dictyostelium. J. Cell Biol.* 109:2841–2851.

Wessels, D., J. Murray, G. Jung, J. Hammer, and D. R. Soll. 1991. Myosin IB null mutant of *Dictyostelium* exhibits abnormalities in motility. *Cell Motil. Cytoskeleton.* 20:301–315.

Wessels, D., J. Murray, and D. R. Soll. 1992. The complex behavior cycle of chemotaxing *Dictyostelium* amoebae is regulated primarily by the temporal dynamics of the natural wave. *Cell Motil. Cytoskeleton.* 23:145–156.

Wessels, D., H. Vawter-Hugart, J. Murray, and D. R. Soll. 1994. Three-dimensional dynamics of pseudopod formation and the regulation of turning during the motility cycle of *Dictyostelium. Cell Motil. Cytoskeleton.* 27:1–12.

Wessels, D., M. Titus, and D. R. Soll. 1996. Dictyostelium myosin I plays a crucial role in regulating the frequency of pseudopods formed on the substratum. *Cell Motil. Cytoskeleton.* In press.

Wuestehube, L. J., and E. J. Luna. 1987. F-actin binds to the cytoplasmic surface of ponticulin, a 17-kD integral glycoprotein from *Dictyostelium discoideum* plasma membranes. *J. Cell Biol.* 105:1741–1751.

Wuestehube, L. J., C. P. Chia, and E. J. Luna. 1989. Immunofluorescence localization of ponticulin in motile cells. *Cell Motil. Cytoskeleton.* 13:245–263.

Zigmond, S. H. 1977. The ability of polymorphonuclear leukocytes to orient in gradients of chemotactic factors. *J. Cell Biol.* 75:606–616.